Hindawi
Geofluids
Volume 2024, Article ID 6637899, 16 pages
https://doi.org/10.1155/2024/6637899

Research Article

A Case Study on Preservation Conditions and Influencing Factors of Shale Gas in the Lower Paleozoic Niutitang Formation, Western Hubei and Hunan, Middle Yangtze Region, China

Shengling Jiang,[1] **Qinghua Zhou**,[2] **Yanju Li**,[1] **and Rili Yang**[1]

[1]*School of New Energy, Longdong University, Qingyang 745000, China*
[2]*Oil and Gas Exploration and Production Branch, China Huadian Green Energy, Co. Ltd., Beijing 100160, China*

Correspondence should be addressed to Shengling Jiang; move824@163.com

Received 7 June 2023; Revised 17 October 2023; Accepted 12 December 2023; Published 8 January 2024

Academic Editor: Shengnan Nancy Chen

The Niutitang Formation of the lower Cambrian (ϵ_1n) is a target reservoir of shale gas widely developed in China's Middle-Upper Yangtze region, with the characteristics of being widely distributed, having a big thickness and highly organic carbon abundance. However, the exploration and research degree are relatively low. Based on extensive core sample, experimental test results, drilling, and field outcrop surveying, the shale gas generation capacity, gas content, and gas composition are discussed. The preservation conditions of shale gas are then systematically analyzed from the aspects of tectonic movement, fault development, structural style, and thermal evolution degree. The results show that the organic-rich shale with a thickness ranging from 40 to 150 m developed in the mid-lower part of the ϵ_1n Formation, with the TOC content values ranging from 0.4% to 14.64%. While it has unfavorable characteristics of a high thermal evolution, with Ro values ranging from 1.92% to 5.74%, a low gas content and a high nitrogen content (70% wells). The ϵ_1n shale gas has complex preservation conditions. The ϵ_1n Formation has good roof-to-floor conditions, but after the main gas generating peak of the ϵ_1n shale during the Jurassic–Cretaceous, the most intensive tectonic activity of the Yanshan movement resulted in poor preservation conditions (faults developed and cap rock fractured). The huge faults extended to the surface are formed due to tectonic movement in an extensional environment, and the structural style and development are the main factors affecting the preservation conditions of the ϵ_1n shale gas. Additionally, the high thermal evolution of the ϵ_1n shales also has a certain impact on the preservation conditions. Therefore, the stable area far from large faults (>2.0 km), with weak local tectonic activity and tectonic deformation, is the favorable area for shale gas preservation in the ϵ_1n Formation.

1. Introduction

The significant advance in shale gas exploration of the Upper Ordovician Wufeng Formation (O_3w)-Lower Silurian Longmaxi Formation (S_1l) in the Sichuan Basin was the first discovery of the Fuling shale gas field [1–3]. The Lower Cambrian Niutitang Formation (ϵ_1n) has a larger resource base than the Wufeng-Longmaxi Formation. The People's Republic of China's Ministry of Natural Resources evaluated the nation's shale gas resources in 2012, and the results showed that the total geological resources were 134.42×10^{12} m^3, of which 39.21×10^{12} m^3 were Cambrian shale gas resources [4], accounting for 29.2% of the total resources. The Southern China's ϵ_1n shale is widely distributed and has a large thickness, with a residual area of approximately 90×10^4 m^2 [5]. The ϵ_1n shale is an organic-rich marine layer formed by sedimentation in shallow water to deep-water continental shelf environments, widely distributed over the Yangtze region.

One of the key areas for shale gas exploration in the Middle-Upper Yangtze region is the Western Hubei and Hunan area. Sixty percent (Hefeng, Laifeng–Xianfeng, Yongshun, Huayuan, Baojing, and Longshan blocks) of the blocks in the Ministry of Natural Resources' second round of shale

gas bidding are all located in this area, but the Western Hubei and Hunan area is a type of basin margin transitional area (around the Sichuan Basin) with complicated geological conditions [6]. Although there has not been a significant advancement in the exploration of shale gas in the Western Hubei and Hunan area, a significant quantity of study has been conducted with ongoing exploration efforts and data collecting. The relevant exploration and study are mainly focused on the O_3w-S_1l shales [7–9]. Studies on $Є_1n$ shale gas mainly concentrated on the sedimentary surroundings [10–12], accumulation conditions [13–15], reservoir characteristics [16, 17], resource potential [18–20], and exploration prospects/directions [21–23]. Previous research achievements show that the $Є_1n$ in Western Hubei and Hunan area is controlled by the sedimentary facies [24]. The black shale is well developed and has a strong material foundation for shale gas generating. Additionally, the $Є_1n$ has experienced a complex thermal evolution history and deep burial process, and it has a high maturity and strong tectonic transformation [6, 25]. As exploration continues to advance and the number of wells drilled continues to rise, it is found that although the $Є_1n$ shale in the basin margin's complex structural area has good static quality, it also shows that the $Є_1n$ shale has a low gas content and high nitrogen composition. The complicated preservation circumstances of the $Є_1n$ shale gas are indicated.

According to earlier research on shale gas in the Sichuan Basin and its environs, the intricate structural evolution process leads to differences in the preservation surroundings for shale gas in different regions [26, 27], and the shale's roof-to-floor conditions and self-sealing properties also control the preservation of natural gas [28]. Generally, the assessment of preservation conditions is mainly carried out from aspects of the tectonic mode and deformation strength, effects of the fracture formation stage, faults and reservoir fracture development, multistage tectonic movement, burial depth surroundings, regional cap rock characteristics, and stratigraphic dip angle [29–33]. And the preservation effect is evaluated from aspects of the pressure coefficient of formation, carbon isotope evidence, shale gas content, geochemical indices, paleofluids, etc. [34–37]. However, previous research regarding the preservation circumstances of the $Є_1n$ shale gas is rare. Only Dong et al. [38], taking well XD1 as an example, preliminarily analyzed the $Є_1n$ shale gas preservation conditions in the Western Hubei by detrital zircon U–Pb technology. Xu et al. [39] studied the preservation conditions of $Є_1n$ shale gas in Western Hubei with respect to structural style, distance between wells and normal faults, fracture development, macroscale sealing of cap rock, thermal evolution degree, burial depth, etc. Therefore, the natural gas preservation conditions of $Є_1n$ shale reservoir in the Western Hubei and Hunan area are thoroughly and methodically discussed based on well data, field outcrop surveys, and sample test data from the aspects of tectonic movement, fault development, structural style, and thermal evolution degree.

2. Geological Setting

Taking into account the tectonic location, the Western Hubei and Hunan fold belt, which is adjacent to the Sichuan Basin, is located in the southeast of the Middle-Upper Yangtze plate, with an area of nearly $5.0 \times 10^4\,km^2$ [8, 40]. The Jiangnan–Xuefeng overthrust uplift belt forms the eastern boundary of the Western Hubei and Hunan fold belt, while the Qinling–Dabie orogenic belt forms the northern boundary [41]. There are five secondary structural units of the Western Hunan and Hubei fold belt from southeast (SE) to northwest (NW), namely, the Sangzhi–Shimen synclinorium belt, Yidou–Hefeng anticlinorium belt, Huaguoping synclinorium belt, Central anticlinorium belt, and Lichuan synclinorium belt (Figure 1). In the study area, there is proof of frequent differential movements influenced by Caledonian and Indo–Chinese movements [42]. The entire area experienced intense deformation as a result of the Yanshan movement, creating faults and folds that trend northeast [43].

The Central Yangtze plate underwent a complete cycle of small- to large-filling scale carbonate sedimentary during the Sinian–Middle Ordovician period. The carbonate sedimentary filling area was shrinking and the clastic rock sedimentary filling area was expanding during the late Ordovician–Silurian. The sedimentary lithology divisions of the Devonian–Carboniferous period are not readily apparent, with the sandstone in the lower section and the carbonate rock in the upper section. Strong similarities were observed between the sedimentary rocks of the Permian–Middle Triassic period, with the main lithological structures of carbonate rocks interbedded with siliceous shale. Therefore, the strata from Proterozoic to Mesozoic in study area developed in different degrees and are dominated by Paleozoic strata and Mesozoic strata with a NE–SW distribution [44].

As the target strata, the $Є_1n$ Formation is distributed over almost the whole studied area. The lithology of the $Є_1n$ lower section is dominated by black carbonaceous shale and carbonaceous siltstone intercalated with carbonaceous micrite limestone, and thin bedded silicates are common in the bottom part, with wavy bedding. The middle section mainly consists of micrite-fine-grained limestone, while the upper section is composed of dark gray thin limestone, black carbonaceous shales, and medium-thick marl. The lithological characteristics of the $Є_1n$ Formation indicate that a rapid regional marine invasion happened in the early Cambrian, the depositional environment was mainly a deep-water continental shelf, and then, the water body gradually shallowed.

3. Samples and Methodology

3.1. Samples. To obtain a relatively comprehensive dataset of the $Є_1n$ shale, the test shale samples were mainly collected in the field sections of Baiguoping, Guchengcun, Yangjiaping, and Jiangpingcun located in the Hefeng area, the Paiwu section and well HY1 located in the Huayuan area, the Wangcun and Mengjiawan sections located in the Yongshun area, and well CY1 located in the Changde area. All shale samples were fresh and unweathered. Nearly 200 samples obtained from two wells and seven sections were tested to obtain the TOC content, Ro, porosity, permeability, Langmuir volume (V_L), field desorption gas content (V_D), and

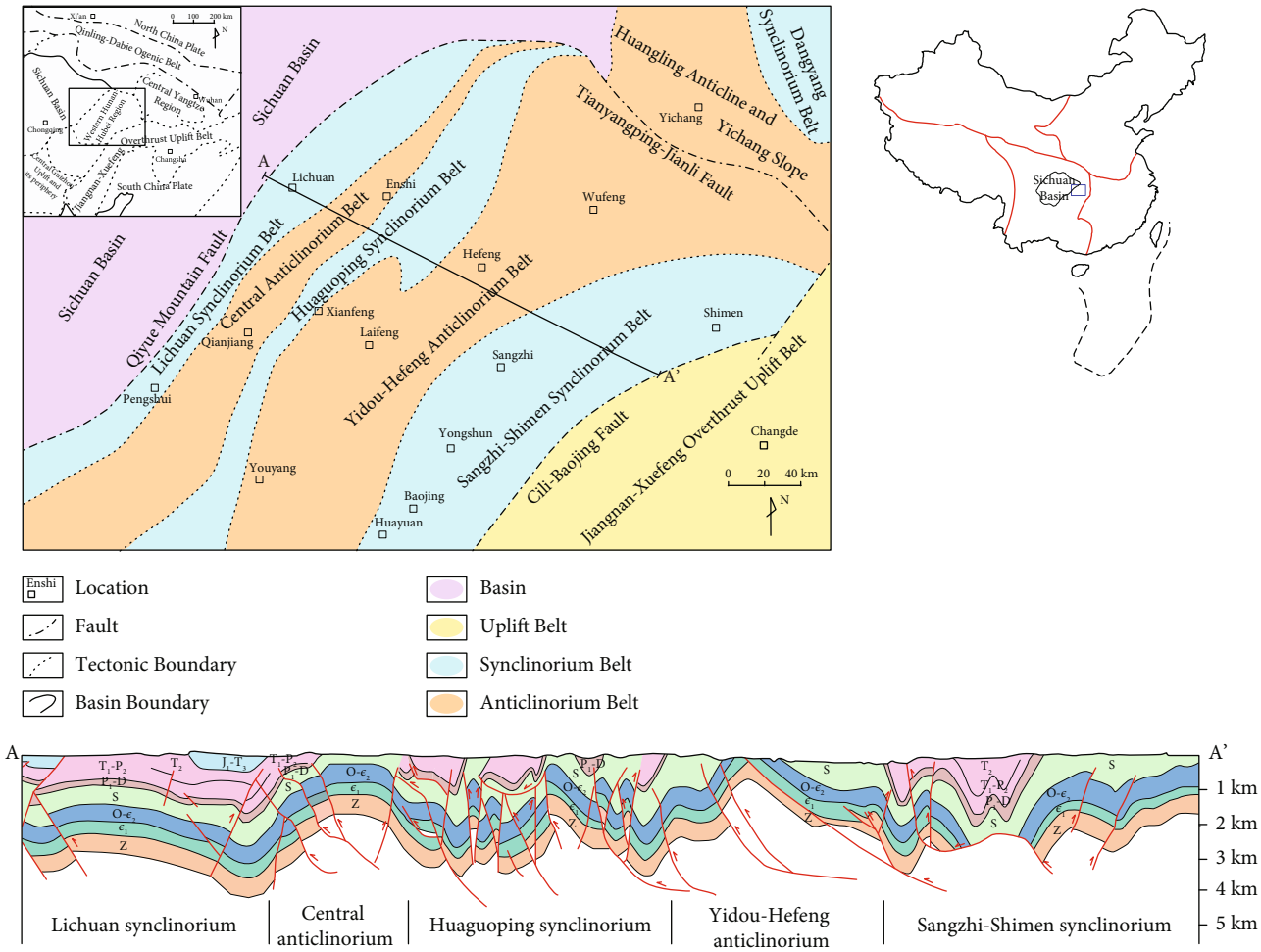

Figure 1: The tectonic division and geological cross-section map of the Western Hubei and Hunan area.

shale gas components. The data of other wells and field sections were mainly obtained from published papers, dissertations, and reports.

3.2. Methodology. The TOC content was determined using a Leco CS-230 carbon-sulfur tester in accordance with the "Chinese National Standard for Determination of Total Organic Carbon in Sedimentary Rock (GB/T19145-2003)." The bitumen reflectance (Br) was measured using a MY9000 digital coal petrography analyzer in accordance with the "Chinese National Standard for Methods to Microscopically Determine the Reflectance of Vitrinite in Sediments (SY/T 5124-2012)." The Br was then converted into the equivalent vitrinite reflectance (Ro) using the formula $Ro = 0.618Br + 0.4$ [44]. Scanning electron microscopy (SEM) was used to measure the pore structures in accordance with the standard of SY/T 5162-2014, and the magnifications ranging from 1000 to 80000 were used to identify the pores and fractures of various sizes. The standard of SY/T 6154-2019 was followed in the quantitative measurement of the pore size.

Using a GAI-100 high-pressure isothermal adsorption apparatus, the V_L representing the shale adsorption capacity was measured in an experimental setting with 1.65% humidity and a constant temperature of 30°C and in accordance with the "Experimental Method of High-Pressure Isothermal Adsorption to Coal (GB/T 19560-2008)" standard. The

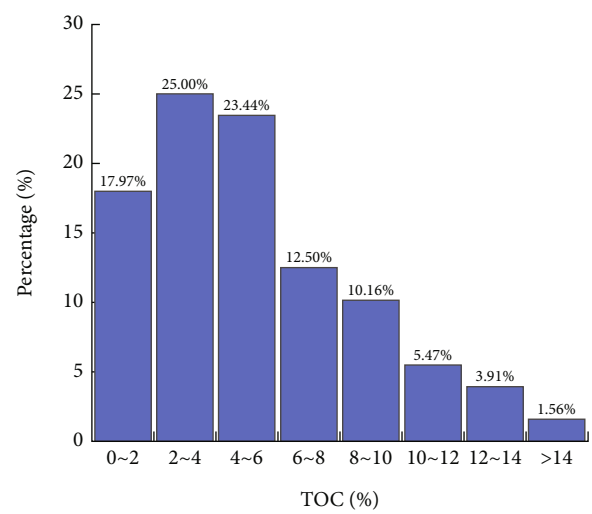

Figure 2: Statistical graph of the $\epsilon_1 n$ shale's TOC content.

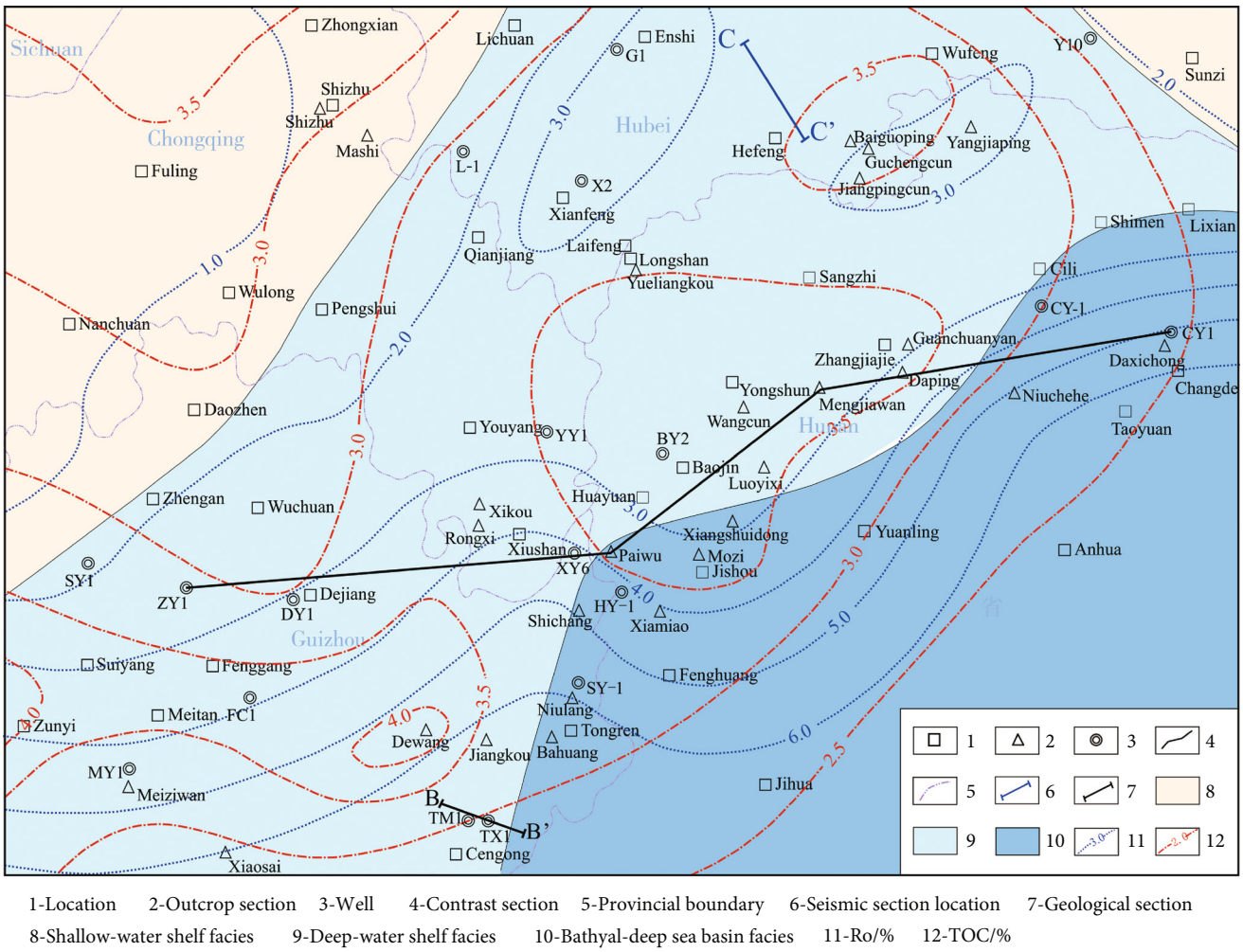

1-Location 2-Outcrop section 3-Well 4-Contrast section 5-Provincial boundary 6-Seismic section location 7-Geological section 8-Shallow-water shelf facies 9-Deep-water shelf facies 10-Bathyal-deep sea basin facies 11-Ro/% 12-TOC/%

Figure 3: Overlay map of the sedimentary facies, TOC content, and Ro of the $\in_1$n shale.

V_D was measured using the field desorption method in accordance with the "Measurement Method of Shale Gas Content (SY/T 6940-2013)" standard. The V_D is made up of three components: the desorption gas volume referred to the gas naturally desorbed from the shale core after the sample canister was sealed under the atmospheric pressure conditions, the lost gas volume recovered from the lifting of the core to the sample filling, and the residual gas volume referred to the gas left in the core sample that was determined by grinding the core sample at a high temperature after the desorption was finished. The shale gas components were tested by a Shimadzu GC-2014C gas chromatograph following the "Analysis of Natural Gas Composition-Gas Chromatography (GB/T 13610-2014)" standard.

The abovementioned samples were all tested by SINOPEC East China Company.

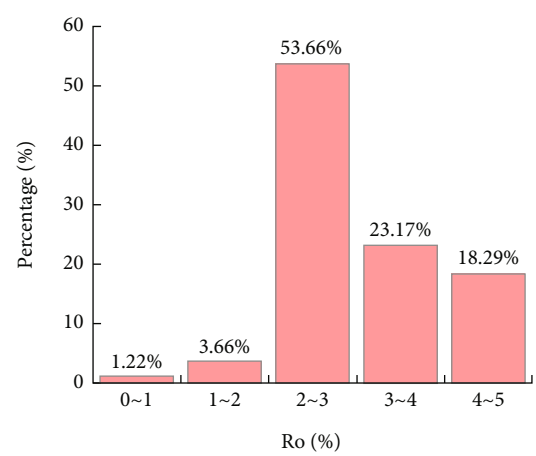

Figure 4: Statistical graph of the $\in_1$n shale's Ro value.

4. Results

4.1. Gas-Generating Capacity of the $\in_1$n Shale. The organic matter abundance is the most basic indicator for evaluating the shales gas-generating capacity. Generally, chloroform asphalt "A" and genetic potential (S_1+S_2) gradually lose their effectiveness with increasing thermal evolution and cannot accurately reflect the original hydrocarbon generation potential [45–47]. The maturity of the $\in_1$n shale in the Western Hubei and Hunan area is high, and it is basically in the high-overmature stage. Therefore, the TOC content

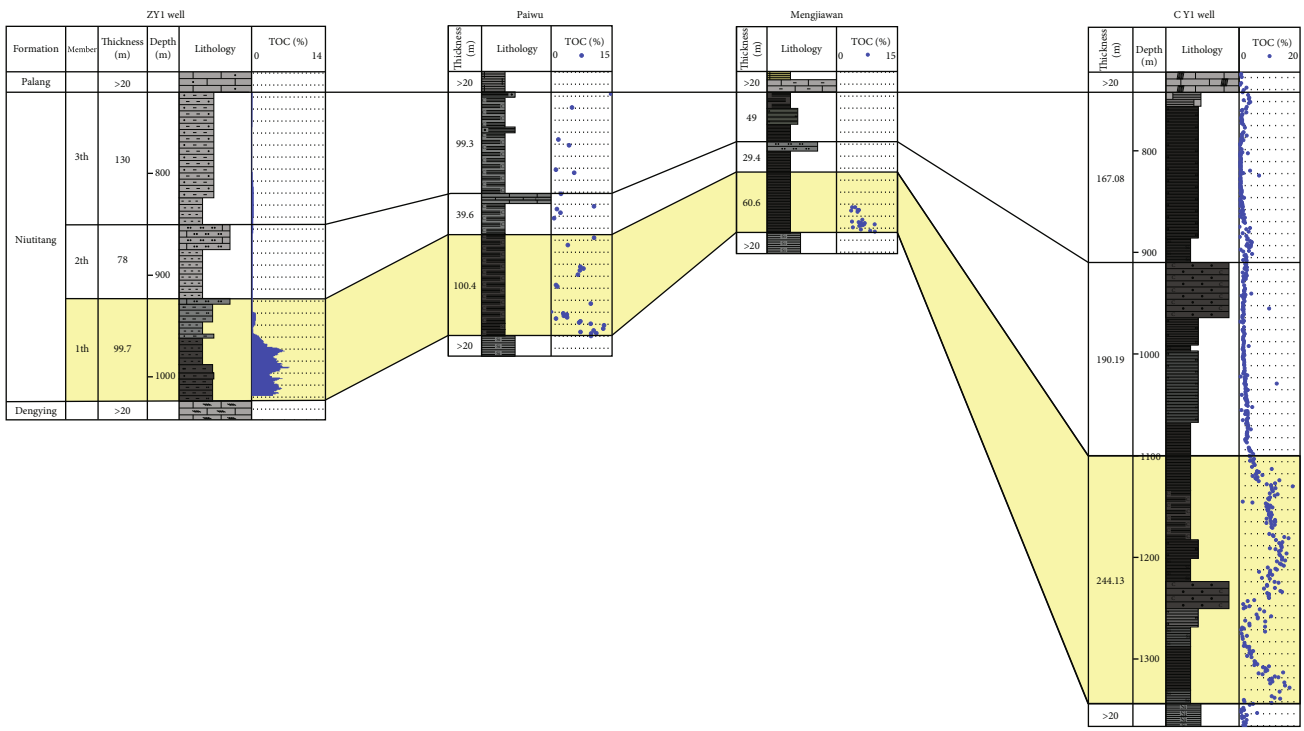

Figure 5: The contrast section of the $\in_1$n shale with TOC > 2.0% (the geological contrast position is shown in Figure 3).

is the greatest important indicator for evaluating shale and its gas-generating capacity.

A total of 128 shale samples from the study area were collected for TOC analysis, and the test findings show that the TOC content ranges between 0.4% and 14.64%, with an average value of 5.23%. Of this, over 82% of the total samples have a TOC content greater than 2.0% (Figure 2), with the main distribution ranging from 2.0% to 8.0%, accounting for 60.94% of the total sample number. The samples with TOC content less than 2.0% account for 17.97%, while which greater than 8.0% accounting for 21.09%. In general, the $\in_1$n shale has a comparatively high TOC content and is evaluated as a high-quality source rock.

Laterally, the trend of TOC content has a close relationship with the sedimentary environment. The TOC content in the Daozhen–Wulong–Shizhu area, with shallow water shelf sedimentary rocks, is approximately 1.0%. In the deep-water shelf sedimentary area, the TOC content in the Youyang–Sangzhi–Wufeng area ranges from 2.0% to 4.0%, and in the bathyal-deep sea sedimentary area, the TOC content reaches its maximum in the Jishou–Changde area, with values ranging from 4.0% to 6.0%. In general, the TOC content increasingly rises from NW to SE in the Western Hubei and Hunan area (Figure 3).

The thermal evolution degree of the $\in_1$n shale in the Western Hubei and Hunan area is high, with the results of 82 shale samples of vitrinite reflectance (Ro) showing that, on average, the Ro value is generally higher than 2.0%, with a main range of 2.0%-5.0%, accounting for 95.12% of the total samples (Figure 4). This suggests that the $\in_1$n shale has reached a high-overmature stage, predominantly generating dry gas. The high thermal evolution characteristics are strongly related to the old age, deep burial depth, and multiple thermal events of the $\in_1$n shale. Laterally, the trend of the Ro value progressively increases from NW to SE in the study area. High Ro value zones have mainly been found in the Jishou–Baojing–Zhangjiajie area and Hefeng–Wufeng area, with Ro values all higher than 3.5% and the maximum values up to 4.13% (Figure 3).

Vertically, the lower section of the $\in_1$n shale has higher TOC content than that in the upper section. The shale section with TOC contents greater than 2.0% is mainly concentrated in the bottom part of the $\in_1$n Formation, which formed in a deep-water shelf and bathyal-deep sea sedimentary environment, with thicknesses ranging from 40 m to 150 m (Figure 5). Taking well CY1 as an example, the $\in_1$n Formation has a thickness of 601.4 m, and the average TOC content is 3.91%, with a range of 0.03% to 17.6%. The TOC content of the lower part of the $\in_1$n Formation is greater than 2.0%, and it has a thickness of 244.13 m and an average TOC content of 6.54%, ranging from 2.0 to 12.0%.

4.2. Gas-Bearing Characteristics of the $\in_1$n Shale

4.2.1. Shale Reservoir Property. In $\in_1$n shale, mainly three different types of pore-fracture structures are developed as organic matter pores, inorganic pores, and microfractures (Figure 6). The organic matter pores are well developed (Figure 6(a)), and the size of which mainly varies in nanoscale. The inorganic pores are mainly interparticle pores distributed among clay particles (Figure 6(b)) and mould pores (Figure 6(d)), and the size of which is overall larger, ranging from several nanometres to micrometres. And a certain

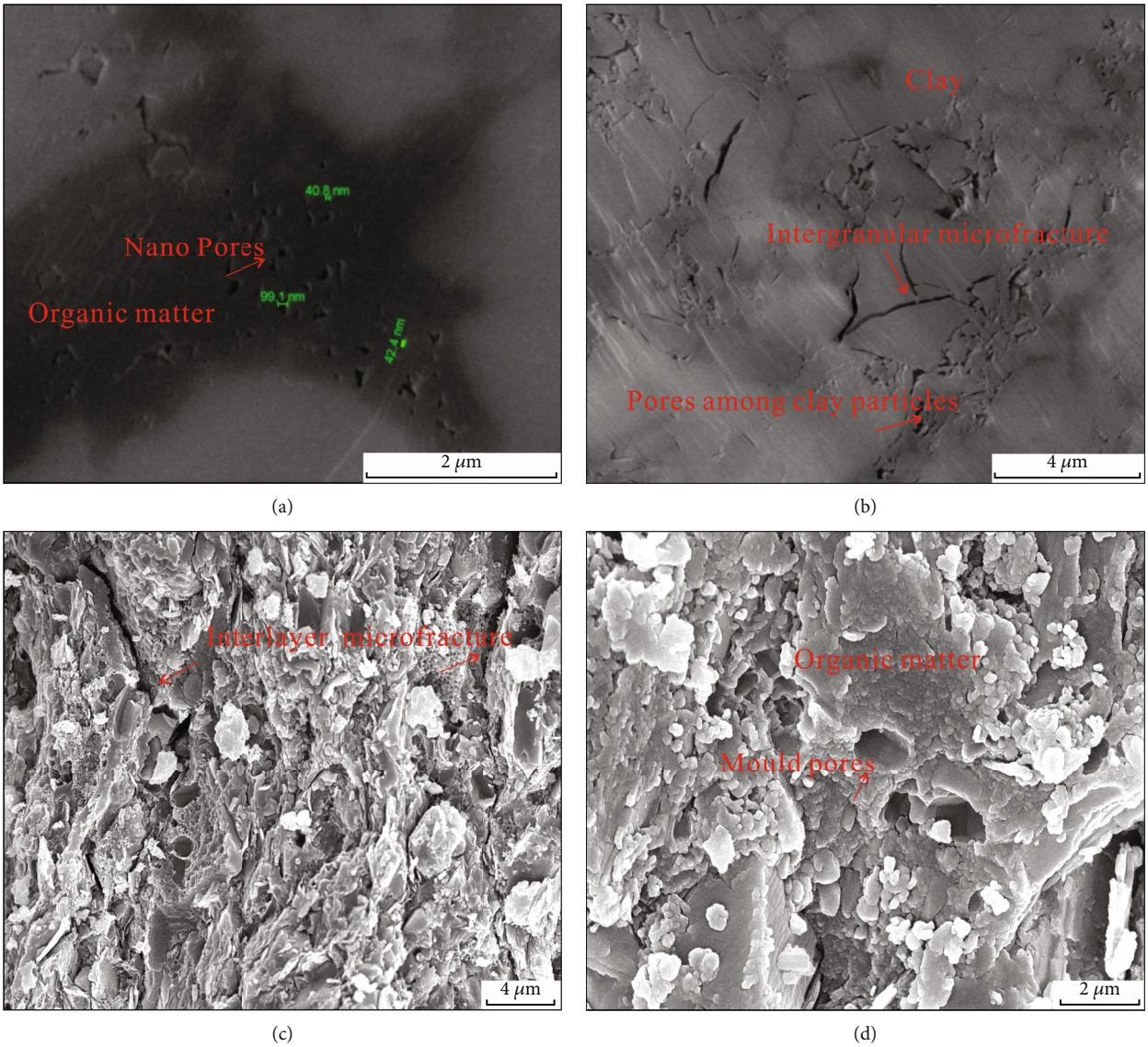

Figure 6: The distribution of $\in_1$n shale's pore-fracture structures in the well HY1: (a) 2461.9 m, organic matter nanopores, ×50000; (b) 2505.2 m, pores among clay particles and intergranular microfracture, ×20000; (c) 2547.8 m, interlayer microfracture, ×3000; (d) 2558.27 m, mould pores in organic matter surface, ×8500.

amount of intergranular microfractures and interlayer microfractures of the $\in_1$n shale developed (Figures 6(b) and 6(c)), the width of which is generally less than 1 μm, and the length ranges from 1 to 16 μm.

The $\in_1$n shale in well HY1 has an average porosity of 0.42% and varied from 0.008% to 1.95%. Of the 34 samples, the porosity of only 12% is greater than 1.0%, and of no samples, it reaches 2.0% (Figure 7). The permeability varies between 0.15×10^{-3} and 4.02×10^{-3} mD, and the average permeability is 0.86×10^{-3} mD. The permeability is all lower than 0.005 mD, which corresponds to the ultra-low-porosity and ultra-low-permeability shale category.

4.2.2. Langmuir Isotherm Adsorption. The isothermal adsorption characteristics of shale are generally described by Langmuir isotherm adsorption curves. The Langmuir

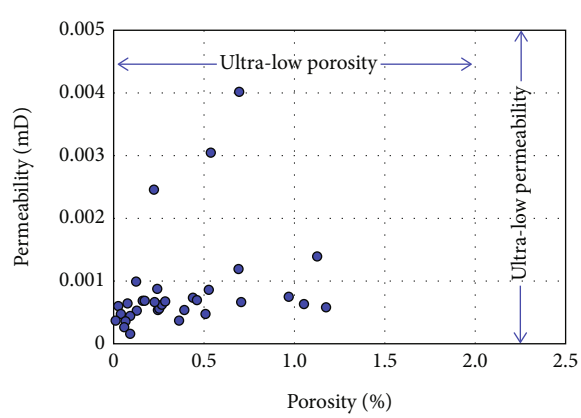

Figure 7: Reservoir properties of $\in_1$n shale in the well HY1.

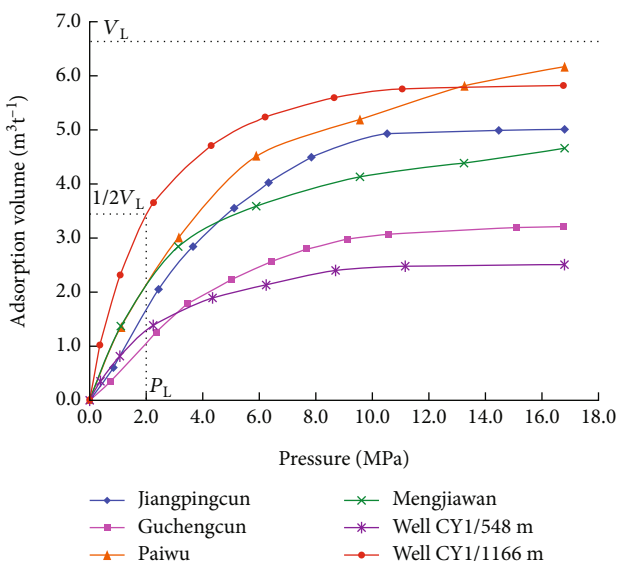

Figure 8: Diagram of Langmuir isotherm adsorption results. Note: V_L—the Langmuir volume at a depth of 1166 m in well CY1; P_L—the Langmuir pressure at a depth of 1166 m in well CY1.

volume (V_L) refers to the theoretical saturated adsorption capacity, which represents the maximum amount of adsorption capacity. When the V_L is halved, the corresponding pressure is the Langmuir pressure (P_L) [48]. The test results show that the average V_L is 3.34 m^3/t, with varying ranges between 1.19 and 7.82 m^3/t. The main distribution range is 1.50-3.80 m^3/t, accounting up to 68% of the samples in total. This indicates that the Є$_1$n shale has a strong capacity for adsorbing methane. The outcrop samples shown in Figure 6 are all taken from the fresh high-quality shale section in the lower part of the Є$_1$n, with V_L varying from 3.2 to 6.60 m^3/t. In well CY1, the V_L of the Є$_1$n shale is 6.87 m^3/t at the depth of 1166 m, which is significantly greater than that of 3.42 m^3/t at the depth of 752 m (Figure 8). This suggests that the lower part of the Є$_1$n shale has a stronger adsorption capacity for methane than other parts.

4.2.3. Field Desorption Experiment. The V_D of the Є$_1$n shale from field desorption experiments is relatively low. According to statistics, the V_D of well YY1 is 0.03-1.12 m^3/t, that of well XY6 is 0.02-2.2 m^3/t [49], that of well CY-1 is 0.32-0.94 m^3/t, that of well BY2 is 0.11-0.71 m^3/t, and that of well HY1 is all lower than 0.029 m^3/t (Table 1). Taking well CY1 as an example, almost 80% of the 51 samples have a V_D between 0 and 0.5 m^3/t, and only 4.0% of the total samples have a V_D higher than 2.0% (Figure 9).

Vertically, the shale section with a relatively higher gas content is developed at the bottom part of the Є$_1$n Formation, and the specific location varies slightly due to different geological conditions. Taking well CY1 as an example, the Є$_1$n black shale was drilled met at the depth of 742.73 m, the Є$_1$n Formation was drilled through at the depth of 1344.13 m, and the completed drilling depth was 1377 m. In well CY1, the V_D of the Є$_1$n shale increases as the burial depth increases. A relatively higher V_D black shale in well CY1 developed at the burial depths ranging from 956 m to 989 m, with a thickness of 30 m and with a V_D ranging from

Table 1: The table of Є$_1$n shale gas composition in wells CY1 and HY1.

Well	Sample ID	CH_4 (%)	C_2H_6 (%)	C_3H_8 (%)	CO_2 (%)	O_2 (%)	N_2 (%)
CY1	CY-1	8.70	0.07	0.00	13.24	1.42	76.57
	CY-2	7.74	0.21	0.00	22.29	2.18	67.58
	CY-3	7.29	0.83	0.00	8.95	4.38	78.55
	CY-4	7.75	0.10	0.01	16.30	3.69	72.15
	CY-5	10.58	0.31	0.01	22.26	2.36	64.48
	CY-6	9.83	0.14	0.00	12.40	4.41	73.22
HY1	HY-1	12.30	0.18	0.00	4.58	0.00	82.94
	HY-2	13.30	0.18	0.00	3.20	0.00	83.32
	HY-3	11.23	0.19	0.00	1.74	0.00	86.84

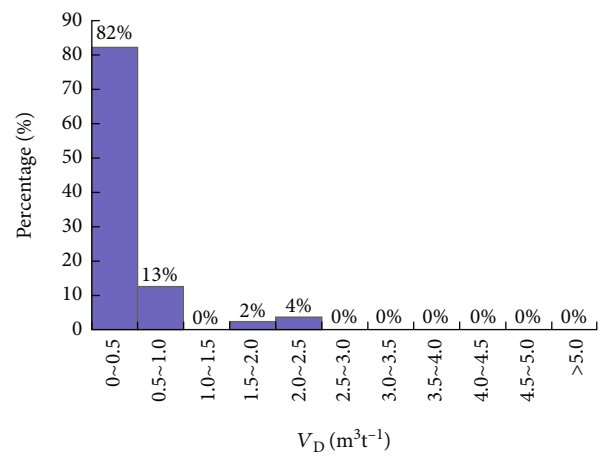

Figure 9: The statistical diagram of V_D in well CY1.

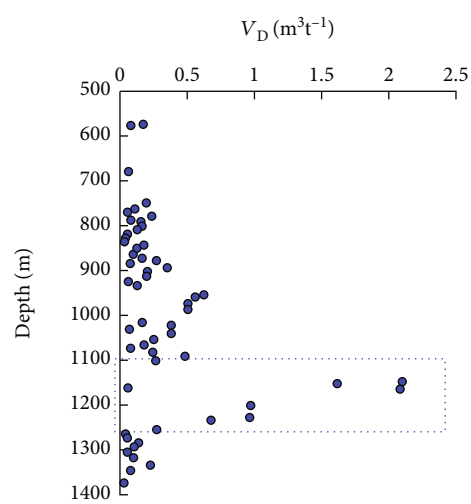

Figure 10: The vertical distribution of V_D in well CY1.

Table 2: The table of the $\in_1$n shale gas composition in study area and its adjacent areas [25, 50].

Location	Well	Gas content ($m^3 \cdot t^{-1}$)	Average N_2 content percentage	Average CH_4 content percentage
Youyang, Chongqing	YY1	0.03-1.12	97.40%	1.20%
	YC1	—	84.10%	15.81%
Xiushan, Chongqing	XY6	0.02-2.2	85.60%	3.86%
Fenggang, Guizhou	FC1	0.4-3.5	84.00%	5.00%
Suiyang, Guizhou	SY1	0.02-0.6	85.36%	13.04%
Meitan, Guizhou	MY1	0.06-0.64	94.62%	4.63%
Cengong, Guizhou	TX1	1.10-2.88	16.20%	79.57%
	TM1	0.1-0.4	>95%	/
Zhengan, Guizhou	ZY1	0.9-2.05	61.37%	6.68%
Suntao, Guizhou	SY-1	0.02-0.85	12.23%	82.20%
Cili, Hunan	CY-1	0.32-0.94	20.00%	80.00%
Changde, Hunan	CY1	0.5-2.1	72.09%	8.65%
Baojin, Hunan	BY2	0.11-0.71	91.45%	8.55%
Huayuan, Hunan	HY1	<0.029	83.87%	12.5%

0.5 to 0.63 m^3/t. The black shale section with the highest gas content developed at the burial depths ranging from 1100 m to 1250 m, with a thickness of 150 m and with a V_D ranging from 0.5 to 2.1 m^3/t. Affected by the occurrence of large cracks in the siliceous rock and siliceous shale, which developed at the bottom part of the $\in_1$n Formation, under strong overthrusting [50], the gas content of the well section at depths of 1250 m to 1344.13 m decreases, with a V_D range of 0.05 m^3/t-0.23 m^3/t (Figure 10). The shale section in well CY1 with a higher V_D is distributed in the upper-middle part of the $\in_1$n Formation's bottom.

4.2.4. Gas Composition. The composition of the 6 shale gas samples from the well CY1 is all mainly N_2, with the N_2 content ranging from 64.48% to 78.55%, with an average of 72.09%. This is followed by CO_2 with a content of 8.95%-22.29%, with an average of 15.90%, and CH_4 with a content of 7.29%-10.58%, with an average value of 8.65%. The average contents of O_2 and C_2H_6 are 3.07% and 2.08%, respectively. There are a few C_3H_8 grains at depths of 1056.3 m and 1230.6 m (Table 1). N_2 also dominates in the composition of the 3 shale gas samples taken from the well HY1 (the N_2 content from the air has been proportionately deducted); the average N_2 content is 83.87%; secondly by CH_4 and CO_2, the average contents are 12.28% and 3.17%, respectively. In general, the N_2 dominates in the shale gas composition of $\in_1$n Formation, and the hydrocarbon gas proportion is relatively low.

The shale gas composition of 14 wells of the $\in_1$n Formation in Western Hunan-Hubei and its adjacent areas were statistically analyzed [50]. The results show that the N_2 contents of 11 wells range from 61.0% to 97.4%, the CH_4 contents of 8 wells are less than 10%, and only 3 wells have high CH_4 contents, ranging from 79.57% to 82.20% (Table 2). The high N_2 content of more than 78% of the wells indicates that the later tectonism and preservation conditions are the key factors for the low gas content and high nitrogen content.

5. Discussion

5.1. Effect of Tectonic Movement on $\in_1$n Shale Gas Preservation. Since the sedimentation of the Cambrian strata, the $\in_1$n shale has gradually entered into the oil generation window in the Caledonian period, with the peak period for oil generation in the late Permian to Middle Triassic period. Natural gas generation began from the period of late Middle–Late Triassic and reached the overmatured stage, which generated dry gas during the middle period of Early Jurassic (Figure 11(a)). The main gas peak of the $\in_1$n shale was during the period of Jurassic–Cretaceous. During this stage, the Western Hubei and Hunan region underwent the most intensive tectonic activity in the Early Yanshanian period, and most areas are greatly uplifted and denuded. The southern area is mainly dominated by thrust nappe structures, whereas central and western areas extremely developed faults. Even the $\in_1$n Formation has undergone the shearing-off and extrusion effect along the layer, resulting in poor shale gas preservation conditions (cap rock fractured and fault developed), and shale gas reservoirs were destroyed (Figure 11(b)). In the Late Yanshanian to Early Himalayan period, the tectonic action has been completely transformed from a compressive tectonic system to an extensional tectonic environment dominated by regional large-scale extension, the strata are further denuded and the large faults developed, which have a significant influence on the shale gas enrichment in $\in_1$n Formation. Strict requirements for shale gas preservation conditions are proposed, especially the area that underwent continuous settlement and burial during the Yanshan III episode of the Late Jurassic to Early Cretaceous, which was favorable for the shale gas preservation, mainly in synclinal areas with less developed faults and sustained subsidence. However, the compression deformation, fold thrusting, uplifting, and denudation during the same geological period were not favorable for the shale gas preservation. In general, the uplift and erosion transformation in the Western Hubei and Hunan area

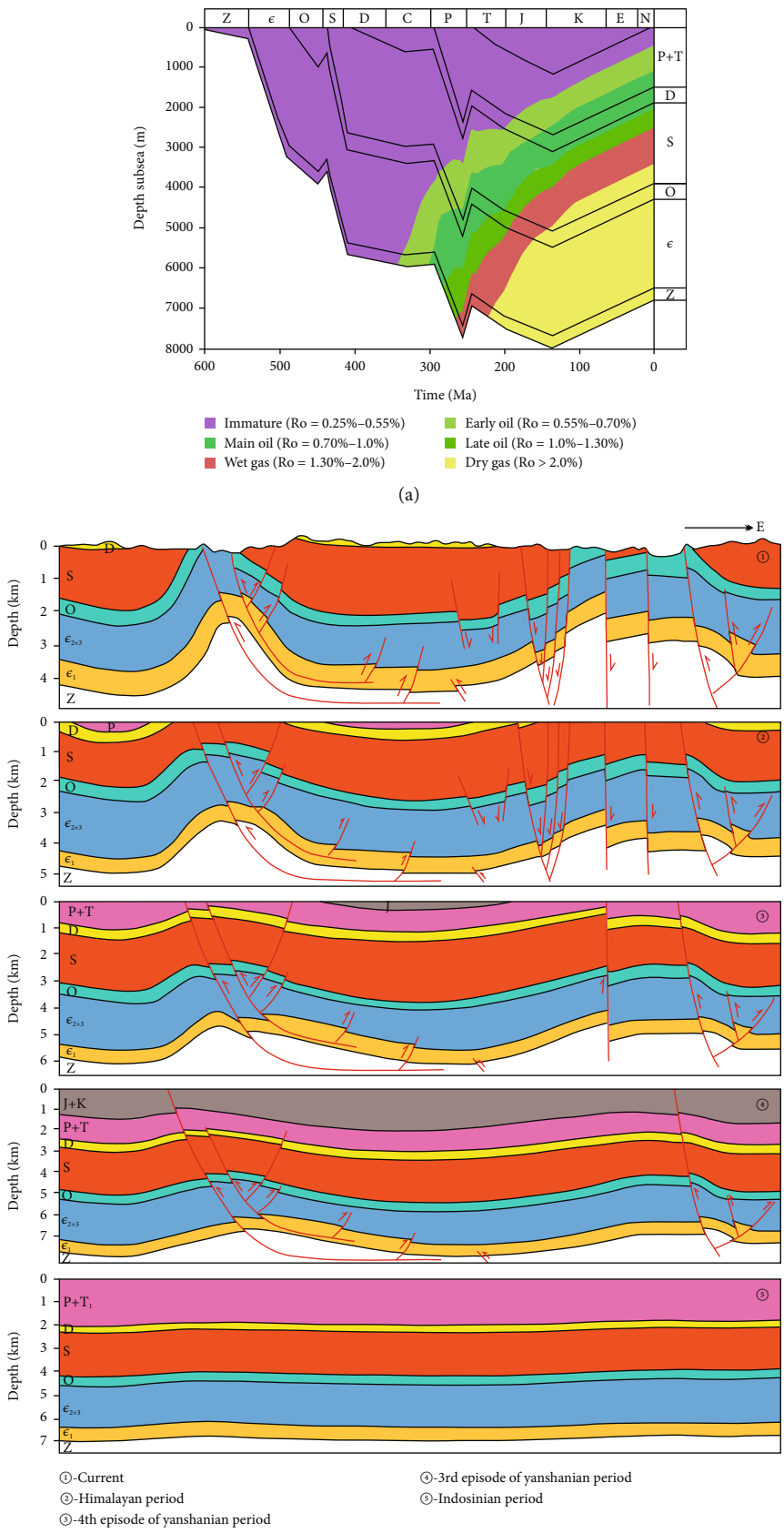

Figure 11: Burial history of the ϵ_1n shale (a) and structural evolution diagram (b) in the Western Hubei and Hunan area.

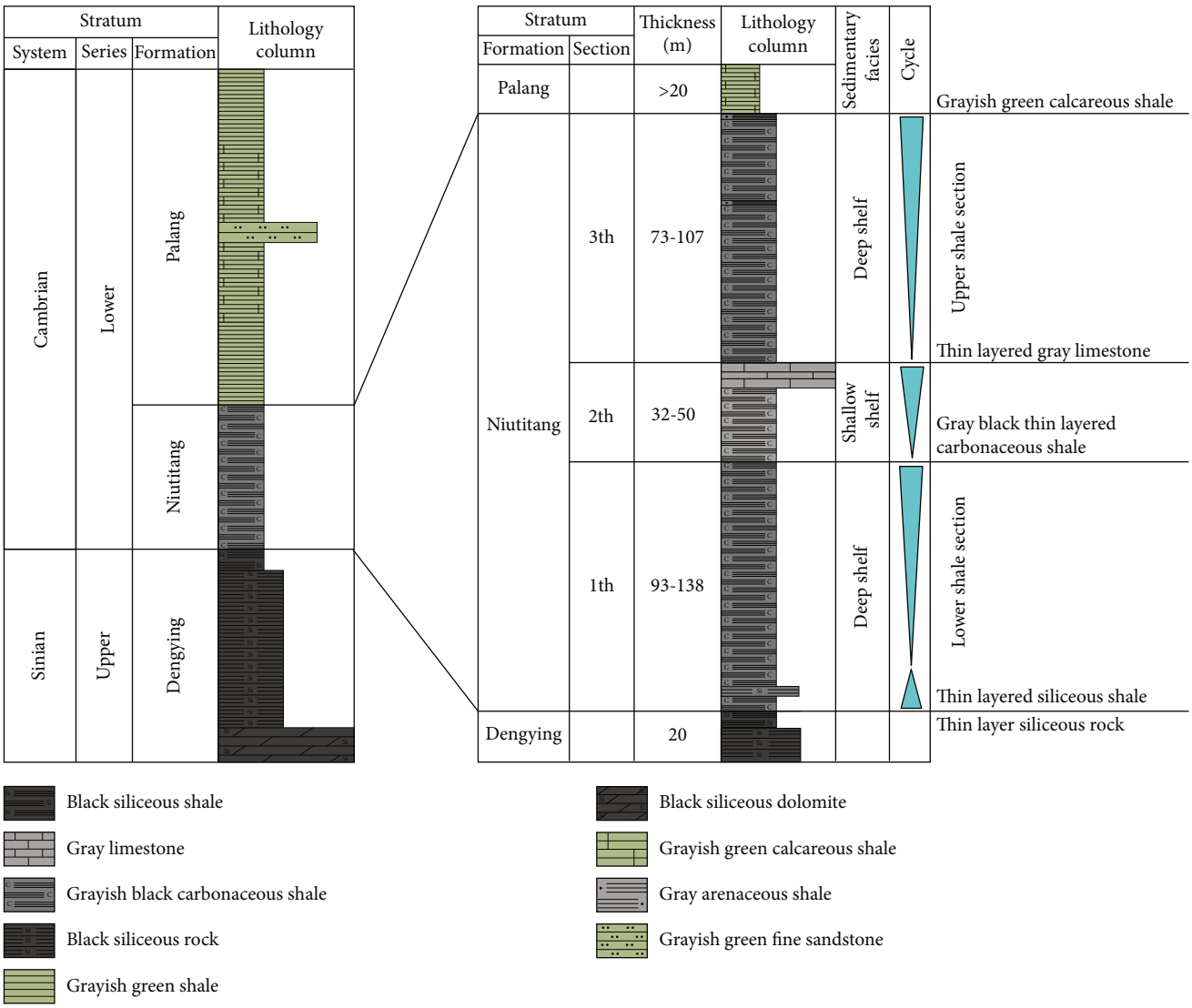

Figure 12: Histogram of roof-to-floor conditions of the ϵ_1n shale in the Western Hubei and Hunan area.

lasted for a long time and were mainly uplifted by folds with large uplift amplitudes. The ϵ_1n shale is exposed in the anticlinorium area [51, 52], but the continuity of the ϵ_1n shale distribution and shale gas preservation conditions is all good in synclinorium area.

5.2. Effect of Roof-to-Floor Conditions on ϵ_1n Shale Gas Preservation. The roof of the ϵ_1n Formation in the Western Hubei area is the Shipai Formation ($\epsilon_1$sp) consisting of gray–green silty shale and pelitic siltstone, occasionally mixed with lenticular or banded marl, with a thickness of 150-200 m, which has good sealing performance. The floor of the ϵ_1n Formation is the Dengying (Z_2dn) Formation composed of grayish white moderately thick micrite dolomite, with a thickness of 250-300 m. Calcite veins and calcite solution pores are often developed through this layer, and cleavage and cracks are relatively developed, so the sealing properties of the Z_2dn Formation are slightly poor.

The roof of the ϵ_1n Formation in the Western Hunan area is the Palang (ϵ_1p) Formation composed of dark gray shale mixed with sandy and calcareous shale, with a thickness of 128-1036 m. The ϵ_1p Formation has good sealing and covering conditions due to its dense lithology. The floor of the ϵ_1n Formation in the Huayuan area, Western Hunan, is the Dengying Formation, consisting of brown and gray thinly layered and dense siliceous rock mixed with siliceous shale, which is an excellent sealing layer with dense lithology. However, in the Yongshun area, the floor is micritic dolomite and argillaceous limestone of the Dengying Formation with characteristics of cleavage and crack development, and its sealing property is relatively poor due to its good permeability.

The high-quality shale with a TOC content higher than 2.0% developed at the bottom part of the ϵ_1n Formation. Taking high-quality shale as an evaluation objective, the upper cover is gray–black thinly layered carbonaceous shale and gray thinly layered limestone of the ϵ_1n Formation's 2nd member and gray–black shale in the upper part of the ϵ_1n Formation (Figure 12). The sealing conditions are good.

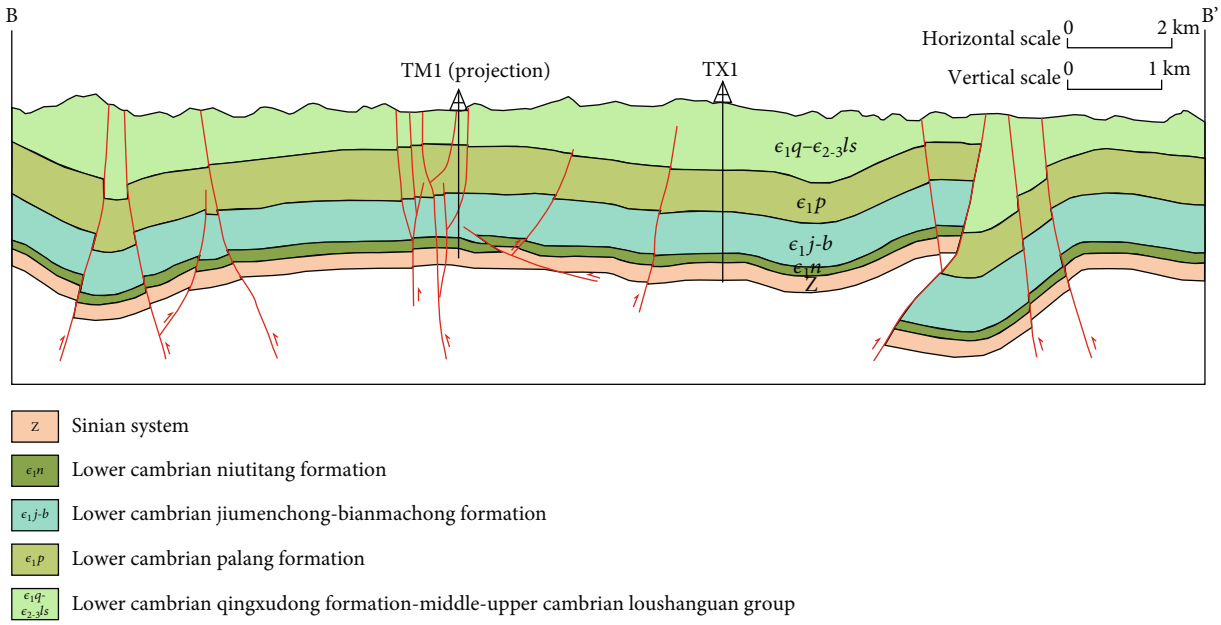

Figure 13: Geological profile of passing well TX1 in Cengong area, northern Guizhou (The plane position is shown in Figure 3).

5.3. Effect of Fault Development on $\epsilon_1 n$ Shale Gas Preservation. The development degree and scale of faults have a significant effect on shale gas enrichment. In particular, large faults that extend outside the shale provide good channels for hydrocarbon expulsion from shale and provide a channel for air to enter the reservoir of shale gas with the atmosphere or formation water acting as a carrier, leading to the shale gas content to decrease and the N_2 content to increase. Therefore, the development of large faults is not conducive to shale gas enrichment. Wells XY6, FC1, BY2, HY1, and CY-1, located in southeastern Chongqing, northern Guizhou, and the Western Hubei and Hunan area, are relatively close to the fault [25]. The ϵ_1n shale is severely affected by the fault, with a low gas content and an average N_2 content of over 84%, especially at well HY1 located in the Bayan syncline and drilled into a fault. The maximum V_D is only 0.029 m^3/t, but the N_2 content of the shale gas is as high as 83.87%. The well TM1 is located in a strike-slip fault zone (Figure 13). There, the ϵ_1n shale has a V_D of only 0.1-0.4 m^3/t and a N_2 content of over 95% [49]. The well TX1 is located in the structurally stability zone, far away from the fault, and the V_D of the ϵ_1n shale is ranging from 1.10 m^3/t to 2.88 m^3/t, with a methane content of 79.57% [50]. At well CY-1 located in the northwest wing of the Jinglongqiao syncline, only small faults have developed, and the V_D of the ϵ_1n shale is relatively low, but the methane content is high, up to 80%.

Influenced by an orogenic belt, the ϵ_1n Formation in the Western Hubei and Hunan area has undergone multiple structural changes, large thrust faults and folds are well developed, and structural units with alternating synclines and anticlines have formed (Figure 14). Complex structural changes and structural patterns will cause damage to the shale gas preservation conditions, causing natural gas to be difficult to accumulate in the shale or in other reservoirs due to the shale gas loss. Meanwhile, the large fracture communicated with the outside causes air to enter the shale, resulting in an increase in N_2 content. However, the structural form is primarily controlled by large thrust fault. Syncline and anticline structural units with clear, complete, and stable distributions are favorable for the shale gas preservation. Therefore, the structural stable area, far from large faults (>2.0 km), of the Western Hubei and Hunan synclinorium is the better enrichment area for ϵ_1n shale gas.

5.4. Effect of Structural Styles on $\epsilon_1 n$ Shale Gas Preservation. According to statistics, the wide, flat, and faulted anticlines and synclines are stable structures with weakly deformed strata that is beneficial for shale gas preservation. However, the complex structure, with the characteristics of strong deformation, great changes in stratum occurrence, fault development, and stratum fragmentation, is unfavorable for shale gas preservation [53]. After the hydrocarbon generation peak, the ϵ_1n Formation underwent three stages of tectonic movements, the Indosinian, Yanshan, and Xishan stages, during which complex structures are formed, such as thrust nappes and strike-slip faults, and extension occurred [54, 55]. Therefore, in the Western Hubei and Hunan area, the complex combinations of destructive residual folds and faults developed. Due to the significant uplift and erosion, strong folds and faults developed, and the structural damaged residual preservation units have poor shale gas preservation conditions. At well HY1, for example, located in the Bayan syncline, southwest edge of the Sangzhi Shimen synclinorium (Figure 15(a)), the maximum V_D of the ϵ_1n shale is only 0.029 m^3/t, a trace amount of gas. However, in areas with weak local tectonic activity and deformation, there are also certain conditions conducive to preservation, such as at wells ZD2, YD2, and YY1 which are located in the wings of the Huanglin anticline, with a

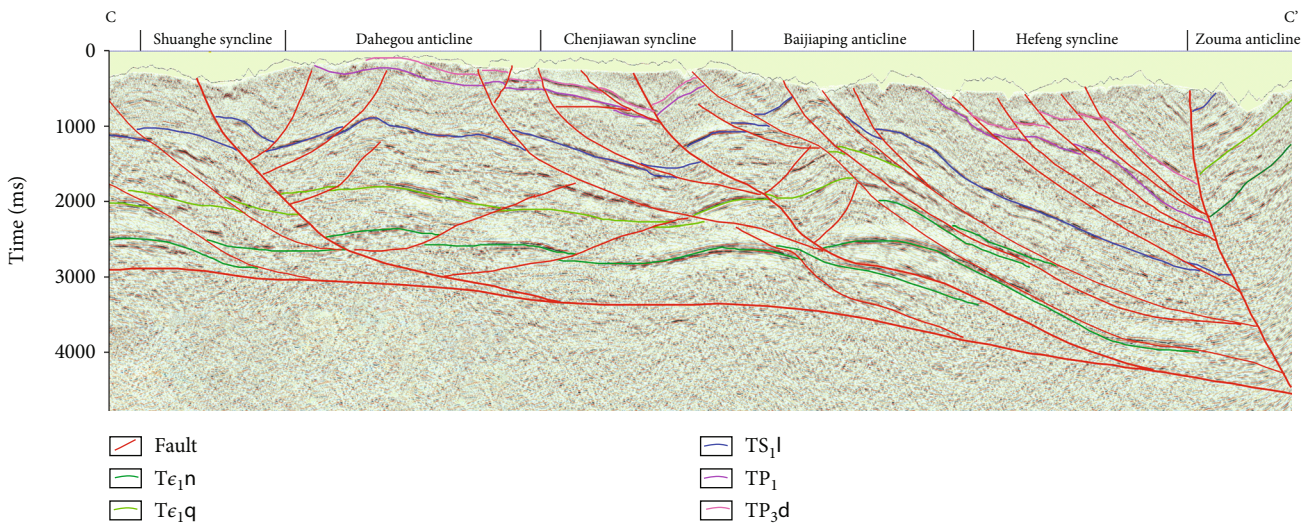

Figure 14: Structure profile of seismic interpretation in Hefeng area, Western Hubei (the plane position is shown in Figure 3). Note: $T\epsilon_1n$—bottom of the lower Cambrian Niutitang Formation; $T\epsilon_1q$—bottom of the lower Cambrian Qinjiamiao Formation; TS_1l—bottom of the lower Silurian Longmaxi Formation; TP_1—bottom of the Permian system; TP_3d—bottom of the upper Permian Dalong Formation.

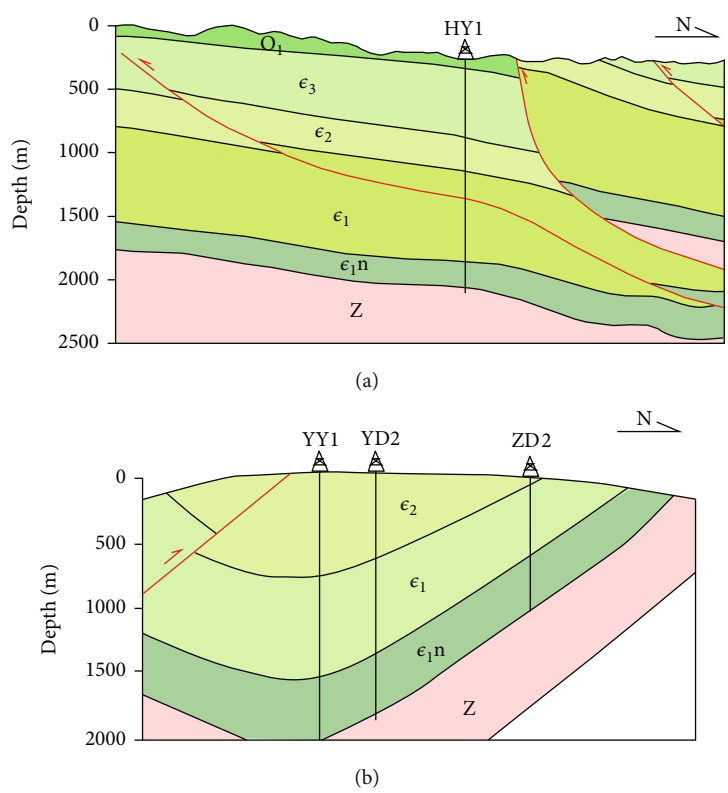

Figure 15: The structure style of well HY1 location (a) and well YY1, YD1 and ZD1 location (b).

V_D of 1.22 m^3/t, 1.54 m^3/t, and 2.05 m^3/t, respectively (Figure 15(b)), and the methane is the major component of the ϵ_1n shale gas [56].

5.5. Effect of Thermal Evolution on ϵ_1n Shale Gas Preservation. On the basis of the shale gas exploration and development experience in the United States, the thermal evolution degree (Ro) of marine shale with organic matter types mainly being type I and type II, thermal origin, and industrial developed shale gas is mainly between 1.1% and 3.0%. When Ro exceeds 3.0%, the shale begins to graphitize gradually, generating a pyrobitumen matrix, and gradually reduces or loses its hydrocarbon generation ability [57, 58]. In addition, the porosity of organic matter shows a trend of first increasing to a peak and then decreasing with increasing Ro. When the maturity is higher than 3.0%, the

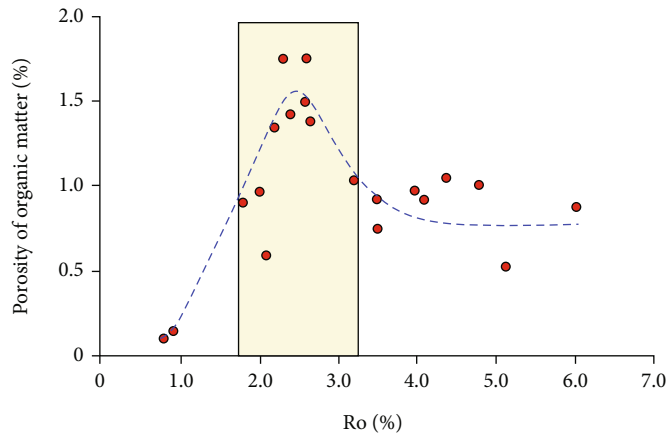

Figure 16: The relationship between Ro and the porosity of organic matter [59].

porosity of organic matter begins to decrease (Figure 16) [59]. As the volume of organic matter micropores decreases, the specific surface area which affected the shale adsorption capacity further decreases, and the maturity also has an impact on the interlayer pores of clay minerals, thereby affecting the shale gas content. The thermal evolution degree of the $\in_1$n shale in Western Hubei and Hunan area is high, with nearly 50% of the samples having an Ro exceeding 3.0%. The main composition of the clay minerals in $\in_1$n shale is illite, which indicates that with increasing maturity and diagenesis, the montmorillonite, illite/smectite mixed layers, and other minerals with large specific surface areas in the $\in_1$n shale have been transformed into illite with small specific surface areas. In general, the thermal evolution degree of the $\in_1$n shale, which is in the stage of overmaturity, late diagenesis, and metamorphism has a certain effect on shale gas content.

6. Conclusion

(1) The $\in_1$n shale in Western Hubei and Hunan area formed in shallow water shelf to deep-water shelf sedimentary environments and is distributed over the whole region, with TOC contents ranging from 0.4% to 14.64% and Ro values generally greater than 2.0%. The organic-rich shale section developed in the middle-lower part of the $\in_1$n Formation, with a thickness of 40-150 m. It is comprehensively evaluated that the shale quality is good and has the material base for shale gas generation

(2) The isothermal adsorption experimental results show that the V_L ranges from 1.19 to 7.82 m^3/t, suggesting that the $\in_1$n shale has a strong natural gas adsorption capacity. The field analysis experiment shows that the $\in_1$n shale generally has low gas content and high N_2 content (78% drillings). The shale gas main component in typical well CY1 and well HY1 is N_2, with average contents of 72.09% and 83.87%, and the average contents of methane are 8.65% and 12.5%, respectively. This shows that the preservation conditions are the critical factor for the enrichment of $\in_1$n shale gas

(3) The $\in_1$n Formation in Western Hubei and Hunan area has good roof-to-floor conditions. The large fault extending to the surface formed in the tectonic movement and tensional environment during the geological history period, and the residual preservation units of structural damage are the mainly factors affecting the $\in_1$n shale gas preservation conditions. Meanwhile, the high thermal evolution degree of the $\in_1$n shale also has a certain impact on $\in_1$n shale gas preservation. In general, the stable area far from large faults (>2.0 km), with weak local tectonic activity and structural deformation, is the favorable area for $\in_1$n shale gas preservation

Data Availability

The data that support the findings of this study are available from the corresponding author upon reasonable request.

Conflicts of Interest

The authors declare no conflicts of interest.

Authors' Contributions

Shengling Jiang was responsible for the writing the original draft and resources. Qinghua Zhou was responsible for the resources. Yanju Li was responsible for the validation. Rili Yang was responsible for the review and editing. All authors have read and agreed to the published version of the manuscript.

Acknowledgments

This research was funded by the Natural Science Foundation of Gansu Province, China (Grant Nos. 22JR5RM202, 23JRRM0760, and 21JR7RM97); the Innovation Foundation of Higher Education in Gansu Province, China (Grant Nos. 2022B-218 and 2023A-141); the Youth Science and

Technology Foundation of Qingyang, China (Grant No. QY-STK-2022A-019); and the Ph.D. Foundation Project in 2020 of Longdong University (Grant No. XYBY202012).

References

[1] K. Zhang, "An analysis of geological structure factor behind the high productivity of Fuling shale gas field and some thoughts," *Sino-Global Energy*, vol. 21, no. 4, pp. 1–8, 2016.

[2] Z. J. Jin, Z. Q. Hu, B. Gao, and J. H. Zhao, "Controlling factors on the enrichment and high productivity of shale gas in the Wufeng-Longmaxi formation, southeastern Sichuan basin," *Earth Science Frontiers*, vol. 23, no. 1, pp. 1–10, 2016.

[3] X. Guo, D. Hu, Y. Li, Z. Wei, X. Wei, and Z. Liu, "Geological factors controlling shale gas enrichment and high production in Fuling shale gas field," *Petroleum Exploration and Development*, vol. 44, no. 4, pp. 513–523, 2017.

[4] D. W. Zhang, Y. X. Li, J. C. Zhang, D. W. Qia O, W. L. Jiang, and J. F. Zhang, *Investigation and Evaluation of Shale Gas Resource Potential in China*, Geological Publishing House, Beijing, 2012.

[5] J. Z. Li, D. Z. Dong, G. S. Cheng, S. Q. Wang, and K. M. Cheng, "Prospects and strategic position of shale gas resources in China," *Natural Gas Industry*, vol. 29, no. 5, pp. 11–16, 2009.

[6] H. L. Liu and H. Y. Wang, "Ultra-low water saturation characteristics and identification of over-pressured play fairway of marine shales in South China," *Natural Gas Industry*, vol. 33, no. 7, pp. 140–144, 2013.

[7] S. J. Jiang, B. Li, C. S. Peng, X. L. Hu, K. Y. Hong, and L. L. Zhu, "Characteristics and gas content of Wufeng-Longmaxi formation shale in the well LD2 of the Laifeng-Xianfeng block," *Geology and Exploration*, vol. 54, no. 1, pp. 203–210, 2018.

[8] S. Jiang, Q. Zhou, Y. Li et al., "Reservoir characteristics and gas-bearing property of Wufeng-Longmaxi shale in well HY2, Hefeng area," *Arabian Journal of Geoscience*, vol. 15, no. 8, 2022.

[9] J. Cai, J. Ji, L. Liu, J. Q. Deng, and K. Li, "Study on shale gas accumulation condition of Upper Ordovivian Wufeng formation-Lower Silurian series Longmaxi formation in Western Hubei and Hunan - Western Hubei and Eastern Chonqing area," *Unconventional Oil & Gas*, vol. 6, pp. 18–24, 2019.

[10] Y. P. Wu, C. L. Liu, H. W. Gong, A. R. Sarwar, H. Yang, and X. X. Zeng, "Geochemical characteristics and sedimentary tectonic setting of the lower Cambrian Niutitang formation in Western Hunan province," *Geology and Exploration*, vol. 57, no. 5, pp. 1065–1076, 2021.

[11] X. Liang, X. Niu, M. Hu, L. Yang, Z. Hu, and Q. Cai, "Development characteristics and sedimentary environment of black shale in the Lower Cambrian Niutitang formation in western Hunan and Hubei," *Lithologic Reservoirs*, vol. 35, 2023.

[12] Q. M. Zhu, L. F. Lu, A. Y. Pan et al., "Sedimentary environment and organic matter enrichment of the lower Cambrian Niutitang formation shale, western Hunan province, China," *Petroleum Geology & Experiment*, vol. 43, no. 5, pp. 797–809, 2021.

[13] K. M. Chen, S. Q. Wang, D. Z. Dong, J. L. Huang, and X. J. Li, "Accumulation conditions of shale gas reservoirs in the Lower Cambrian Qiongzhusi formation, the Upper Yangtze region," *Natural Gas Industry*, vol. 29, no. 5, pp. 40–44, 2009.

[14] H. Nie, J. Zhang, and Y. Li, "Accumulation conditions of the lower Cambrian shale gas in the Sichuan basin and its periphery," *Acta Petrolei Sinica*, vol. 32, no. 6, pp. 959–967, 2011.

[15] M. Y. Hu, Q. J. Deng, and Z. G. Hu, "Shale gas accumulation conditions of the lower Cambrian Niutitang formation in upper Yangze region," *Oil & Gas Geology*, vol. 35, no. 2, pp. 272–279, 2014.

[16] H. Li, X. H. Chen, Z. Q. Peng, L. Chen, A. Liu, and S. Y. Luo, "Shale gas reservoir characteristics of the lower Cambrian Niutitang formation in the western Hunan and Hubei areas," *Acta Geologica Sinica*, vol. 96, no. 4, pp. 1421–1433, 2022.

[17] Y. Y. Guo, M. L. Liang, Z. X. Wang, L. Y. Zhang, H. J. Li, and X. S. Li, "Organic geochemistry and mineral composition characteristics in shales of Niutitang formation, Northwestern Hunan," *Journal of Geomechanics*, vol. 25, no. 3, pp. 392–399, 2019.

[18] Y. K. Long, "Lower Paleozoic shale gas exploration potential in central Yangze area, China," *Geological Bulletin of China*, vol. 30, no. 2/3, pp. 344–348, 2011.

[19] B. Chen and Z. K. Lan, "Lower Cambrian shale gas resource potential in upper Yangtze region," *China Petroleum Exploration*, vol. 14, no. 3, p. 10, 2009.

[20] L. Yue, Y. Kang, Q. Chen, Y. Shang, Z. She, and L. Chen, "Analysis of shale gas potential of Niutitang formation of Lower Cambrian in Guizhou, China," *Xinjiang Petroleum Geology*, vol. 34, no. 2, pp. 123–128, 2013.

[21] P. W. Wang, C. Zou, Y. Z. Liu et al., "Shale gas exploration prospect evaluation in the Hefeng block of the Western Hubei and Hunan provinces," *Geological Science and Technology Information*, vol. 33, no. 6, pp. 104–109, 2014.

[22] J. Wang, C. Zou, and W. M. Huang, "The shale gas exploration propect assess of the Niutitang formation in western Hubei and Hunan- eastern Chongqing," *Geological Science and Technology Information*, vol. 23, no. 4, pp. 98–102, 2014.

[23] Y. Jihong, L. Qigui, and Z. Xiang, "Main factors controlling shale gas accumulation and exploration targets in the lower Cambrian, Sichuan basin and its periphery," *Petroleum Geology & Experiment*, vol. 38, no. 4, pp. 445–452, 2016.

[24] Y. Wang, J. Chen, L. Hu, and Y. M. Zhu, "Sedimentary environment control on shale gas reservoir: a case study of lower Cambrian Qiongzhusi formation in the middle lower Yangtze area," *Journal of China Coal Society*, vol. 38, no. 5, pp. 845–850, 2013.

[25] Y. F. Wang, J. G. Leng, P. Li, and F. Li, "Characteristics and its main enrichment controlling factors of shale gas of the lower Cambrian Niutitang formation in northeastern Guizhou province," *Journal of Palaeogeography*, vol. 18, no. 4, pp. 605–614, 2016.

[26] Y. Ma, X. Cai, and P. Zhao, "China's shale gas exploration and development: understanding and practice," *Petroleum Exploration and Development*, vol. 45, no. 4, pp. 589–603, 2018.

[27] X. He, Y. Gao, X. Tang, P. Zhang, and G. He, "Analysis of major factors controlling the accumulation in normal pressure shale gas in the southeast of Chongqing," *Natural Gas Geoscience*, vol. 28, no. 4, pp. 654–664, 2017.

[28] H. K. Nie, Z. L. He, G. X. Liu et al., "Status and direction of shale gas exploration and development in China," *Journal of China University of Mining & Technology*, vol. 49, no. 1, pp. 13–35, 2020.

[29] Y. Zhang, Y. J. Li, L. Pan, R. S. Yu, and Y. T. Zhang, "The influence of structural characteristics on the preservation

conditions of shale gas in Nanchuan area, Chongqing," *Geological Bulletin of China*, vol. 42, no. 5, pp. 680–686, 2023.

[30] J. Li, H. Li, C. Yang, Y. Wu, Z. Gao, and S. Jiang, "Geological characteristics and controlling factors of deep shale gas enrichment of the Wufeng-Longmaxi formation in the southern Sichuan basin, China," *Lithosphere*, vol. 2022, no. 12, Article ID 4737801, 2022.

[31] W. X. Guo, J. M. Tang, J. S. Ouyang, T. Wang, X. Wang, and Y. Wang, "Characteristics of structural deformation in the southern Sichuan basin and its relationship with the storage condition of shale gas," *Natural Gas Industry*, vol. 41, no. 5, pp. 11–19, 2021.

[32] J. Li, H. Li, C. Yang, X. Ren, and Y. Li, "Geological characteristics of deep shale gas and their effects on shale fracability in the Wufeng-Longmaxi formations of the southern Sichuan basin, China," *Lithosphere*, vol. 2023, no. 1, 2023.

[33] X. Wei, Y. Li, Z. Wei, R. Liu, G. Yu, and Q. Wang, "Effects of preservation conditions on enrichment and high yield of shale gas in Sichuan basin and its periphery," *Petroleum Geology & Experiment*, vol. 39, no. 2, pp. 147–153, 2017.

[34] H. Li, J. Zhou, X. Mou et al., "Pore structure and fractal characteristics of the marine shale of the Longmaxi formation in the Changning area, southern Sichuan basin, China," *Frontiers in Earth Science*, vol. 10, 2022.

[35] K. Lu, Y. H. Huang, S. He et al., "Indication of geochemical indexes for shale gas preservation conditions in shale fractures vein: evidence from Yangzi Permian organic-rich shale in the Leping formation," *Natural Gas Geoscience*, vol. 34, no. 6, pp. 1090–1102, 2023.

[36] A. Liu, Q. Wang, X. Chen et al., "Geochemical characteristics of paleo-fluids in thrust belt in the northern middle Yangze and its significance for shale gas preservation: a case study of well Baodi 1," *Petroleum Geology & Experiment*, vol. 44, no. 4, pp. 620–628, 2022.

[37] H. Nie, C. Sun, P. Li et al., "Carbon isotope evidence for shale gas preservation conditions and large methane release over million years: a case study of shale gas reservoirs of Wufeng and Longmaxi Formations in the Sichuan Basin," *Geoscience Frontiers*, vol. 14, no. 6, article 101642, 2023.

[38] M. Dong, L. Y. Zhang, Z. X. Wang, H. Dong, and Y. G. Zhu, "Accumulation characteristics and preservation conditions of Niutitang formation of lower Cambrian series shale gas in West Hubei: a case study of well XD1," *Earth Science*, vol. 44, no. 11, pp. 3616–3627, 2019.

[39] L. L. Xu, X. H. Zhou, W. Chen et al., "A study on shale gas preservational conditions of the lower Cambrian Niutitang formation in the western Hubei," *Marine Origin Petroleum Geology*, vol. 26, no. 2, pp. 113–122, 2021.

[40] H. Li, Y. S. Bai, B. Z. Wang, and G. T. Zhang, "Preservation conditions research on shale gas in the lower Paleozoic of western Huan and Hubeiarea," *Petroleum Geology and Recovery Efficiency*, vol. 21, no. 6, pp. 22–26, 2014.

[41] F. Yang and J. Z. Ye, *Structural Characteristics and Shale Gas Exploration Potential in Southeast Sichuan-Western Hubei and Hunan Areas*, China University of Geosciences Press, Wuhan, 2011.

[42] Q. Z. Wang, F. Yang, and Y. S. Yu, "Analysis on the relationship between tectonic evolution and shale gas preservation in southeastern Sichuan-western Hunan and Hubei region," *Journal of Yangtze University*, vol. 9, no. 4, pp. 44–46, 2012.

[43] B. Li, G. Q. Wei, K. Y. Hong, C. S. Peng, X. L. Hu, and L. L. Zhu, "Evaluation and understanding on the shale gas wells in complex tectonic provinces outside Sichuan Basin, South China: a case study from well Laiye 1 in Laifeng-Xianfeng block, Hubei," *Natural Gas Industry*, vol. 36, no. 8, pp. 29–35, 2016.

[44] H. Jacob and J. R. Song, "Migration bitumen," *Natural Gas Exploration and Development*, vol. 3, pp. 81–87, 1986.

[45] S. S. Hao, F. Y. Wang, G. Gao, and W. Z. Gang, "Characteristics and evaluation of the lower Paleozoic high-overmature source rock," *China Petroleum Exploration*, vol. 2, no. 1, pp. 25–32, 1996.

[46] D. G. Liang, T. L. Guo, J. P. Chen, L. Z. Bian, and Z. Zhao, "Several new developments in marine hydrocarbon generation and accumulation in southern China: distribution of four sets of regional marine source rocks in southern China," *Marine Petroleum Geology*, vol. 17, no. 2, pp. 1–16, 2008.

[47] P. Yang, Y. Xie, X. Li, D. Bai, Z. Liu, and H. Chen, "Hydrocarbon-generating potential of the source rocks of the Sinian Doushantuo formation on the western side of the Xuefeng Mountain," *Geology in China*, vol. 39, no. 5, pp. 1299–1309, 2012.

[48] D. J. K. Ross and R. M. Bustin, "Impact of mass balance calculations on adsorption capacities in microporous shale gas reservoirs," *Fuel*, vol. 86, no. 17-18, pp. 2696–2706, 2007.

[49] T. Lin, J. C. Zhang, S. J. Bao, Y. S. Yu, B. Li, and W. He, "The optimum selecting of shale gas well location and gas content of lower Cambrian, Northwest Hunan: a case study of well Changye," *Natural Gas Geoscience*, vol. 26, no. 2, pp. 312–319, 2015.

[50] R. Wang, W. Ding, D. Gong et al., "Gas preservation conditions of marine shale in northern Guizhou area: a case study of the lower Cambrian Niutitang formation in the Cen'gong block, Guizhou Province," *Oil& Gas Geology*, vol. 37, no. 1, pp. 45–55, 2016.

[51] Y. Wo, Y. Zhou, and K. Xiao, "The burial history and models for hydrocarbon generation and evolution in the marine strata in southern China," *Sedimentary Geology and Tethyan Geology*, vol. 19, no. 3, pp. 280–294, 2012.

[52] H. K. Nie, S. J. Bao, B. Gao et al., "A study of shale gas preservation conditions for the Lower Paleozoic in Sichuan basin and its periphery," *Earth Science Frontiers*, vol. 19, no. 3, pp. 280–294, 2012.

[53] Y. Shu, Y. C. Lu, H. Y. Bao, C. Wang, and Z. H. Liu, "Three typical types of shale gas preservation in the Fuling shale gas field, Sichuan basin," *Natural Gas Industry*, vol. 38, no. 3, pp. 31–40, 2018.

[54] Y. S. Ma, Z. H. Lou, T. L. Guo, X. Y. Fu, and A. M. Jin, "An exploration on a technological evalua-tion for marine system of petroleum preservationstrata in South China," *Acta Geologica Sinica*, vol. 80, no. 3, pp. 406–417, 2006.

[55] Y. M. Chen, X. X. Gao, and X. C. Shen, "Tectonic evolution characteristics and mechanism in western Hunan-Hubei," *Oil Geophysical Prospecting*, vol. 48, Supplement 1, pp. 157–162, 2013.

[56] L. Xu, S. Huang, Z. Liu et al., "Geological controls of shale gas accumulation and enrichment mechanism in Lower Cambrian Niutitang formation of western Hubei, Middle Yangtze, China," *Frontiers in Earth Science*, vol. 15, no. 2, pp. 310–331, 2021.

[57] R. M. Pollastro, D. M. Jarvie, R. J. Hill, and C. W. Adams, "Geologic framework of the Mississippian Barnett shale,

Barnett-Paleozoic total petroleum system, bend arch-Fort Worth Basin, Texas," *AAPG Bulletin*, vol. 91, no. 4, pp. 405–436, 2007.

[58] D. H. Li, J. Z. Li, S. J. Wang, and X. J. Li, "Analysis of controls on gas shale reservoirs," *Natural Gas Industry*, vol. 29, no. 5, pp. 22–26, 2009.

[59] W. F. Fan, D. J. Hou, and Y. Liang, "Comparative study on reservoir forming conditions between Niutitang and Longmaxi formation of shale gas in South China: taking Southeast Chongqing area for example," *Science Technology and Engineering*, vol. 15, no. 27, pp. 13–22, 2015.